Biophysical Chemistry 144 (2009) 72–77

Contents lists available at ScienceDirect

Biophysical Chemistry

journal homepage: http://www.elsevier.com/locate/biophyschem

Single molecular dynamic interactions between glycophorin A and lectin as probed by atomic force microscopy

Chao Yan [a,1], Alexandre Yersin [a], Rehana Afrin [a,b], Hiroshi Sekiguchi [a], Atsushi Ikai [a,c,*]

[a] Laboratory of Biodynamics, Graduate School of Bioscience and Biotechnology, Tokyo Institute of Technology, 4259 Nagatsuta, Midori-ku, Yokohama, Kanagawa 226-8501, Japan
[b] Biofrontier Center, Tokyo Institute of Technology, 4259 Nagatsuta, Midori-ku, Yokohama, Kanagawa 226-8501, Japan
[c] Innovation Laboratory, Tokyo Institute of Technology, 4259 Nagatsuta, Midori-ku, Yokohama, Kanagawa 226-8501, Japan

ARTICLE INFO

Article history:
Received 25 May 2009
Received in revised form 25 June 2009
Accepted 25 June 2009
Available online 2 July 2009

Keywords:
Glycophorin A (GpA)
Psathyrella velutina lectin (PVL)
Atomic force microscope (AFM)
Protein–protein interaction
Dynamic force spectroscopy
Membrane protein

ABSTRACT

Glycophorin A (GpA) is one of the most abundant transmembrane proteins in human erythrocytes and its interaction with lectins has been studied as model systems for erythrocyte related biological processes. We performed a force measurement study using the force mode of atomic force microscopy (AFM) to investigate the single molecular level biophysical mechanisms involved in GpA-lectin interactions. GpA was mounted on a mica surface or natively presented on the erythrocyte membrane and probed with an AFM tip coated with the monomeric but multivalent *Psathyrella velutina* lectin (PVL) through covalent crosslinkers. A dynamic force spectroscopy study revealed similar interaction properties in both cases, with the unbinding force centering around 60 pN with a weak loading rate dependence. Hence we identified the presence of one energy barrier in the unbinding process. Force profile analysis showed that more than 70% of GpAs are free of cytoskeletal associations in agreement with previous reports.

1. Introduction

Most biological processes are achieved through direct molecular interactions whose specificity and strength are determined by the chemical, physical and mechanical properties of the participating molecules. An important example of such molecular interactions can be found in the signal transduction pathway from the outside to the inside of a living cell [1]. This kind of signal transduction plays a fundamental role in the modulation of cellular activities and development of pathological states due to diseases. The topic transmembrane protein, glycophorin A (GpA), has been demonstrated as a specific receptor for Sendai virus [2], malaria parasites (*Plasmodium falciparum*) [3], and *Escherichia coli* hemolysin [4] as three representative pathogenic agents. Such observations stimulated our interest greatly and prompted us to elucidate the biophysical basis of the interactions between GpA and a lectin as a model ligand of GpA. Recent technological development of AFM has brought us to an unprecedented advantage so that we can explore the fundamental mechanisms of life processes directly at the single molecular level under physiological conditions [5]. This novel approach will greatly deepen our understanding of the processes involving membrane receptors and extra-cellular ligand molecules as well as the related biological structures providing interesting hints for new therapeutic approaches.

GpA is a 131-amino acid, highly glycosylated sialoglycoprotein that spans the erythrocyte plasma membrane once and presents its amino-terminal end on the extra-cellular surface [6]. It contains approximately 15 *O*-glycans, the carbohydrates covalently attached to the hydroxyl group of serine or threonine, and one *N*-glycan, the carbohydrate covalently bound to asparagine through an amide linkage [7]. The major *O*-glycan in GpA is the tetrasaccharide NeuAcα2-3Galß1-3 (NeuAcα2-6) GalNAcα together with its truncated forms as minor components [8], and pentaoligosaccharides that contains three sialic acid residues (e.g. Neu5Ac) [9]. Two polymorphic variants of GpA present M and N epitopes in human and give rise to the MN blood groups [6]. GpA monomers are normally dimerized in the form of juxtaposed α-helices within the plasma membrane and each erythrocyte has about $5.0–9.0 \times 10^5$ copies of GpA [10]. PVL is a lectin from the fruiting body of *Psathyrella velutina*, which can recognize two kinds of non-reducing terminal carbohydrate epitopes, *i.e.*, GlcNAc and Neu5Ac residues in GpA [11,12]. It is a monomeric lectin with 401 amino acid residues. Its crystal structure is given in PDB as 2bwr, for example. It is a multivalent lectin and can bind up to six ligands in a monomeric unit.

The interactions between GpA and PVL have been studied by Krotkiewska et al. [13] using a BIAcore biosensor equipped with a surface plasmon resonance detector. They found that the binding constants of immobilized PVL with native GpA were similar to each other, regardless of the blood group of erythrocytes as the source of

* Corresponding author. Innovation Laboratory, Tokyo Institute of Technology, 4259 Nagatsuta, Midori-ku, Yokohama, Kanagawa 226-8501, Japan. Tel./fax: +81 45 924 5828.
E-mail address: ikai.a.aa@m.titech.ac.jp (A. Ikai).
[1] Chao Yan's present address: S9 Bld. 806, Quantum Nanoelectronics Research Center, Tokyo Institute of Technology. 2-12-1 Ookayama, Meguro-ku, Tokyo 152-8550, Japan.

0301-4622/$ – see front matter © 2009 Elsevier B.V. All rights reserved.
doi:10.1016/j.bpc.2009.06.009

the GpA samples. The stationary unbinding force on the red blood cell has been measured by Afrin et al. [14] to be around 70 pN by AFM. However, no data are available for the dynamics of GpA–PVL interactions and the availability of such data will be important for understanding the mechanism of GpA–PVL complex formation and the way the recognition process proceeds.

In order to investigate the GpA–PVL interactions at the molecular level, we designed dynamic force spectroscopy experiments *in vitro* as well as *in situ* for comparison, and analyzed the force curves obtained in the force-volume mode of AFM using Bell-Evans model [1,15,16]. Interaction mechanics between macromolecular ligands and receptors has been an important target of AFM studies and many examples together with the fundamentals of force spectroscopy are extensively covered by Butt et al. [5]. Examples of such studies, especially using lectins as a receptor and glycoproteins as ligands, are found in [17–19]. By adopting similar methodologies, we found that the dissociation reaction of GpA-PVL complex was defined by a single energy barrier within the experimentally accessible range of the force loading rate in this work. Measured results for *in vitro* and *in situ* experiments showed that similar binding and unbinding events were taking place under the two different conditions. We also performed an inhibition experiment to verify the specificity of the reaction. A further force profile analysis showed that most GpAs are free of direct cytoskeletal association in agreement with previous reports. The erythrocyte membrane contains other glycoproteins, such as glycophorin B and C with similar sugar moieties with GpA but the latter is the predominant species on the molar basis. Another major glycoprotein on the erythrocyte membrane, Band 3, has only a few terminal sialic acids but no terminal *N*-acetyl glucosamines [20]. We, therefore, considered the *in situ* force data presented in this paper were mainly on GpA. The experimental approach developed here can also be applied to investigate the interactions between GpA and other lectins.

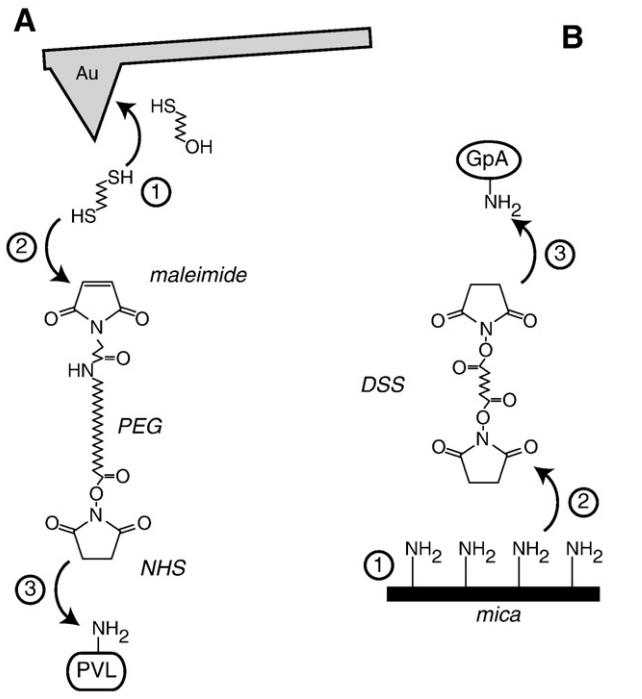

Fig. 1. Three-step cross-linking protocol for AFM tip and mica substrate. (A) First, gold-coated tips were modified by incubation with 1, 8-octanedithiol (1 mM) and 6-mercapto hexan-1-ol. Second, a heterobifunctional PEG linker was anchored to amino-group bearing tips through maleimide end. Third, PVL was finally cross-linked to tip by attaching to the NHS free end of PEG. (B) First, mica was aminosilanized by exposure to APTES vapors. Second, DSS was attached to amino-group through one of its NHS ester end. Third, GpA was cross-linked finally by interaction between its amino group end and the other NHS ester end of DSS.

2. Materials and methods

2.1. Chemicals and proteins

APTES (3-aminopropyltriethoxysilane), DIPEA (*N, N*-diisopropylethylamine), 1,8-octanedithiol, 6-mercapto hexan-1-ol, CHAPS (3-[(3-cholamidopropyl) dimethylammonio]-1-propanesulfonate) and bovine GpA was purchased from Sigma-Aldrich, (St. Louis, MO). DSS (disuccinimidyl suberate) was supplied by Pierce (Rockford, IL) and the PEG crosslinker, *N*-hydroxy-succinimide ester-polyethlene glycol-maleimide (NHS-PEG-MAL) with the PEG part of 3400 Da was purchased from Nektar Therapeutics (Huntsville, AL). The lectin, PVL, was purchased from Wako Chemicals (Tokyo, Japan). Phosphate buffered saline without extra calcium ions (PBS (-)) was supplied from Gibco Invitrogen (Carlsbad, CA).

2.2. Preparation of mica substrate and AFM cantilever

Mica substrates with a diameter of 9.9 mm were purchased from Ted Pella Inc. (Redding, CA). Commercial soft cantilever probes, OMCL-TR400 PB-1 (both sides gold coated) with a nominal force constant of 0.02 nN/nm and extremely soft gold coated cantilevers, BL-RC-150VB, with a nominal force constant of 0.006 nN/nm were both provided by Olympus (Tokyo, Japan). The cantilever force constants were determined by thermal noise analysis [21], with an uncertainty range of approximately ±10%. Cross-linking of PVL and GpA to cantilever tips and mica substrates respectively was a three-step process as schematized in Fig. 1.

First, cantilevers and mica substrates were cleaned in a UV ozone cleaner (NL-UV253, Nippon Laser & Electronics Lab., Japan). Then mica substrates were silanized by exposing them to APTES vapors for 2 h in a 2-liter desiccator filled with argon and containing 30 µl APTES and 10 µl DIPEA in small vessels to introduce primary amino groups to mica surface [22,23]. Cantilevers were incubated with 50 µl of 2 mM 1,8-octanedithiol and 50 µl of 20 mM 6-mercapto hexan-1-ol in ethanol for more than 18 h to introduce thiol-groups on the tip surface. The modified cantilevers with thiol groups were washed with ethanol and incubated for 60 min with 1 mg/ml of NHS-PEG-MAL in PBS. They were then washed several times with PBS to remove unreacted crosslinkers.

Second, the amino silanized mica was incubated in a 2–2.5 mM DSS dissolved in 2.5% DMSO solution in ethanol for 60 min and then rinsed with MilliQ water for 3 times to remove unreacted DSS. Third, the DSS modified pieces of mica as above were incubated with 0.2–1 mg/ml GpA dissolved in an aqueous CHAPS solution (50 mg/ml) for 60–90 min while the NHS-PEG-MAL modified cantilevers as above were incubated in an aqueous solution of PVL (0.2–1 mg/ml) for 60–90 min. Finally modified cantilevers and mica substrates were extensively washed with PBS (pH 7.4) to remove unbound molecules and CHAPS micelles for force measurement. Forced removal of unbound GpA from the mica surface in 1% sodium dodecyl sulfate solution in PBS was sometimes used without significant difference in the results.

2.3. Red blood cell

Erythrocytes were collected from fresh human blood by 5 min centrifugation at 2000 RPM and then subjected to centrifugal washing for five times with PBS supplemented with 2 mM ATP. An aliquot of diluted cell suspension in PBS was left on a poly-L-lysine-coated slide glass for 30 min and then gently rinsed with the same buffer just before force measurement experiments.

2.4. AFM force measurement

All the force measurements for *in vitro* experiments were performed with a commercial NanoScope III MultiMode AFM (Digital Instruments, Santa Barbara CA), and for *in situ* experiments we used a BioScope AFM (Veeco, Plainview, NY) which enabled us to monitor the location of the AFM cantilever over the cell surface through an optical microscope. In the force volume mode, the tip was alternately approached to and retracted from 16×16 points over a 1 μm^2 sample surface while force curves were synchronously recorded. Dynamic force spectroscopy study was achieved by varying the retraction speed of cantilever from 100 to 7500 nm/s and its ramp size from 100 nm to 200 nm. The hydrodynamic drag force should not interfere the force measurement significantly as long as it is working on the cantilever under steady state conditions.

2.5. Data analysis

We analyzed force curves with software developed on a fuzzy logic algorithm [24]. Most probable unbinding force was obtained by applying a Gaussian fitting curve multiplied by a window function to the histogram of unbinding force in order to account for the limited force sensitivity [25,26]. The apparent loading rate was defined as the slope of the force curve just before the final rupture event. Errors in the determination of the mean of the distribution and in the cantilever spring constant uncertainty were taken into account as the uncertainties in the mean unbinding force and in the loading rate. Mean rupture length histograms were obtained similarly while the uncertainty was given by the standard error of the mean. Detailed description of this method can be found in our previous publication [27].

3. Results

3.1. Most probable unbinding force study

We started our investigation of GpA–PVL interactions of *in vitro* experiment first, in which PVL was cross-linked to an AFM tip and GpA was mounted on a flat mica substrate as described above and schematically shown in Fig. 1. Force distance curves were recorded in PBS (pH 7.4) under the force-volume mode of the multimode AFM while a basic media was supplied to mimic extracellular environments in which the interaction of GpA and its lectins usually occurs. A collection of recorded typical force-distance curves in the retraction regime is given in Fig. 2(A). The cantilever started retracting from the substrate surface at the leftmost end of the curves, initially following a straight line and then followed by a distinctly non-linear force extension profile characteristic to the stretching of PEG linkers until a rupture event (a force curve jump) took place, where a sudden upward deflection of the tip was recorded. The numerical value of the rupture force can be calculated by multiplying the deflection change in nm by the cantilever force constant in nN/nm. While some retraction curves showed no indications for specific GpA–PVL interactions, approximately 40–50% of all the curves presented a typical feature of an abrupt upward deflection ended with a jump of the cantilever to its free position, which was interpreted as representing the rupture event of specific GpA–PVL interaction. The magnitude of this force jump was taken as the force required to unbind the GpA–PVL complex, which was confirmed by control experiments given below. For each approaching and retracting speed of the tip to the sample, N (generally $N = 2048$) curves were recorded over different spots while the tip was scanning over the sample surface. The typical force curves were extracted, analyzed and plotted into a force histogram (Fig. 2(B)) by Matlab based fuzzy logic algorithm as described above. In order to avoid possible inclusion of non-specific adhesion events, only those rupture events taking place after 10 nm extension of PEG linkers were collected in the given histograms here and elsewhere in this paper.

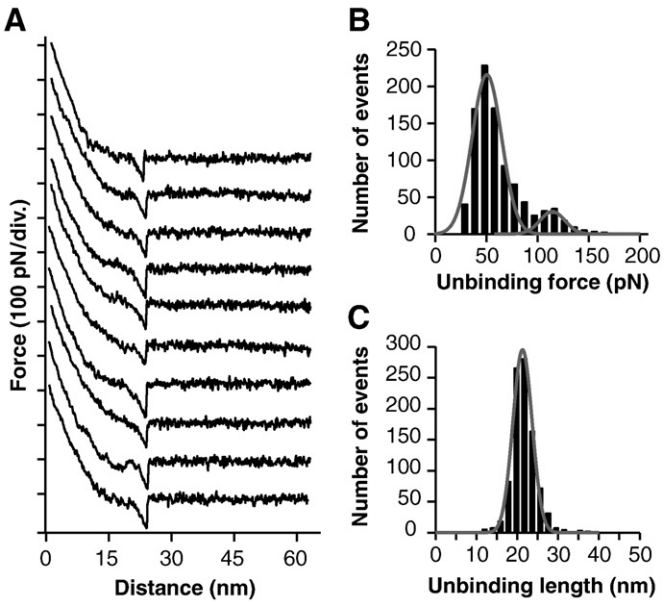

Fig. 2. Specific interaction between purified GpA and PVL for *in vitro* experiment. (A) Typical interaction force curves measured on mica. Vertical axis indicates cantilever deflection as a function of the cantilever-substrate retraction distance. (B) Force histogram of 923 unbinding events out of 2048 force curves. The mean unbinding force value is 52 ± 14 pN at a mean loading rate of 0.9 nN/s. (C) Unbinding length distribution corresponding to the events shown in B, centered at 22 ± 6 nm.

A clear major peak arose from the Gaussian fitting of the force distribution with a mean and a standard deviation of 52 pN and 14 pN, respectively, at a mean loading rate of 0.9 nN/s. The mean unbinding length for these events was Gaussian fitted to be 22 ± 6 nm (Fig. 2(C)), which corresponded to the extension of the PEG linker modeled as a worm like chain of 30 nm contour length under a tensile force of 60 pN [5]. A minor peak under the second Gaussian fitting curve was considered as the result of multiple unbinding events.

We then proceeded to *in situ* experiments following the same procedure using similarly functionalized tips to probe the native GpA molecules directly over erythrocytes surface on the BioScope AFM. Force curves were recorded, analyzed and plotted into a histogram in Fig. 3, in the same way as with *in vitro* experiments. Typical force curves (16.5%) were featured with extremely long cantilever deflection up to 620 nm before the force curve jump occurred, which was considered to come mainly from the extension of the cell membrane, otherwise known as tether formation [14]. From Gaussian fitting curve of the histogram of the final unbinding force given in the inset of Fig. 3, the most probable unbinding force was obtained as 63 ± 9 pN under a loading rate of 14.5 nN/s.

3.2. Dynamic force spectroscopy analysis

By recording force curves with various tip speeds (consequently different loading rates), we found that the most probable unbinding force was not a constant for GpA–PVL pair but depends on the loading rate of the pulling force. The measured loading rate range was from 0.135 nN/s to 9 nN/s for *in vitro* experiment and from 1.35 nN/s to 40.5 nN/s for *in situ* experiment, with corresponding most probable unbinding force values varying from 42 to 60 pN, and from 50 to 65 pN, respectively. This feature of GpA-lectin interactions is an example of dynamic force spectroscopy, which plots the values of most probable unbinding force against the logarithm of apparent loading rate, as schematized in Fig. 4(A).

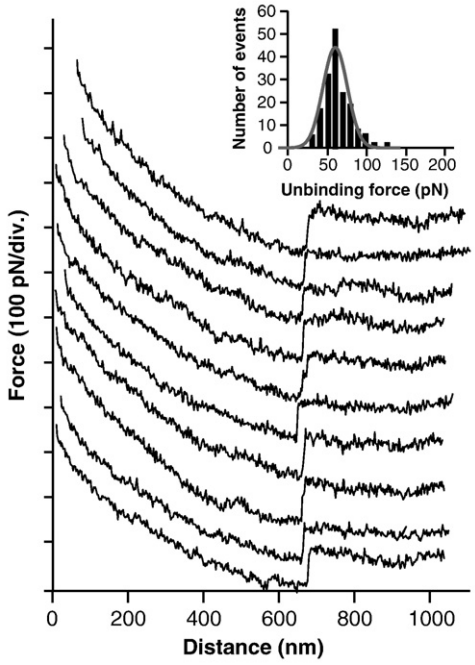

Fig. 3. Typical interaction force curves recorded *in situ*. They are featured with the long extension. Inset on upper right is the force histogram of 169 unbinding events out of 1024 force curves. The mean unbinding force value is 63 ± 9 pN at a mean loading rate of 14.5 nN/s, with unbinding probability of 16.5%.

The results fitted well with a commonly adopted Bell-Evans model in describing unbinding pathway of molecular interactions, where the transition from bound to unbound state is described as the escaping process of the bond from a potential well by overcoming one or more activation energy barriers [15,16]. When a constant external force, f, is applied to a GpA–PVL pair, the dissociation process is facilitated by a lowered energy barrier resulting in an increased dissociation rate constant as:

$$k_d(f) = k_d^0 exp\left(\frac{f\Delta x}{k_B T}\right) \quad (1)$$

where k_d^0 is the intrinsic dissociation rate (i.e., dissociation rate constant under zero external force), Δx is the width of the energy barrier (the distance between the maximum and minimum of the interaction potential) along the direction of applied force, k_B is the Boltzmann constant and T is temperature in Kelvin. When the applied force increases with a constant rate r_f, the most probable unbinding force, f^*, can be written as:

$$f^* = \frac{k_B T}{\Delta x} ln \frac{\Delta x}{k_d^0 k_B T} + \frac{k_B T}{\Delta x} ln\left(r_f\right) \quad (2)$$

By curve fitting, we found that the dynamic properties of GpA–PVL interaction was almost the same for both *in vitro* and *in situ* experiment, as shown in Fig. 4(A). It shows that only one rate regime exists, in which the force increases linearly with the force loading rate. Parameters concerning GpA–PVL interaction can be calculated by applying experimental data to Eq. (2).The values of Δx and k_d^0 were obtained as 0.990 nm and 1.4×10^{-3} s^{-1}, respectively. This value is in reasonable agreement with the reported value of 3.45×10^{-3} s^{-1} for the interaction between PVL and fetuin and 2.39×10^{-3} s^{-1} for PVL and asialoagalactofetuin [28]. With the reported dissociation constant K_D of GpA–PVL as 4.3 nM [13], the association rate constant k_a^0 can be obtained as 3.3×10^5 mol^{-1} s^{-1} which is also in good agreement with the reported value of $1.35\times10^5 mol^{-1}$ s^{-1} for PVL-fetuin and $4.6\times10^5 mol^{-1}$ s^{-1} for PVL-asialoagalactofetuin interactions [28]. It is interesting to note that our calculated rate constants for PVL–GpA interaction are closer to those reported for PVL-asialoagalactofetuin than for PVL-fetuin interaction. Finally an approximate geometry of energy landscape for GpA–PVL interaction was depicted in Fig. 4(B) with only one activation barrier at a position 0.990 nm from the equilibrium bond length.

3.3. Specificity of unbinding force

In order to confirm the specificity and our interpretation of the measured unbinding event, we did the unbinding length study and inhibition experiment.

3.3.1. Unbinding length study

An important evidence to support the interpretation of unbinding force as the force needed to break GpA–PVL complex came from an inhibition experiment and measurement of unbinding length, which mainly determined by cross-linker extension from zero distance to the position of the complex rupture in a force-distance curve. The contour length of the extended PEG linkers was estimated to be about 32 nm according to its molecular weight [29]. The measured unbinding lengths based on over 2000 rupture events were in the rage from 20–30 nm, as one example shown in Fig. 2(C), which strongly supported the interpretation of a rupture event as breaking specific interactions between GpA and PVL. This is a reasonable value because the PEG linker was extensible up to 70–80% of its contour length at the tensile force of ~60–70 pN.

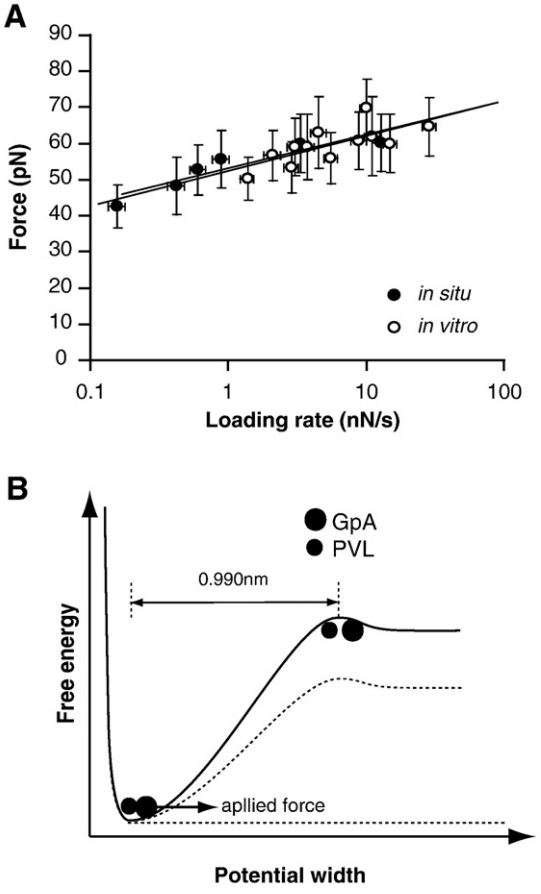

Fig. 4. Dynamic interactions between GpA and PVL. (A) Dynamic force spectroscopy of GpA–PVL interactions *in vitro* (white dots) and *in situ* (black dots). The most probable unbinding force was plotted as a function of the loading rate logarithm, which showed that only one regime exists for GpA and PVL interactions. Solid lines represent the fitting curves corresponding to Eq. (2). Error bars were obtained as described in Data analysis part. (B) Energy landscape. Only one energy barrier exists for GpA–PVL complex to overcome from bound state to unbound state at a distance of 0.990 nm from the equilibrium bond length.

3.3.2. Inhibition experiment

An inhibition experiment was designed in which force measurement was performed with a large excess of free GpA in solution. Binding of free GpA molecules to PVL on tip should prevent the formation of a complex during approach of the tip to surface and thus no rupture event was expected. In one set of experiment, the force measurement was, first, conducted without inhibition and result was obtained that unbinding force of 52 ± 14 pN (Fig. 2(B)) and binding probability of 46% at the loading rate of 0.9 nN/s. Then keeping all other experimental conditions unchanged, a large excess of free GpA was added to the solution on the mica surface, which was washed with PBS (pH 7.4) before force measurement. The results of such experiments are given in Fig. 5(A) and (B) where the binding probability dropped to about 1% in the presence of free GpA, demonstrating that our measurement was precisely targeted on the interactions between GpA and PVL with little interference of non-specific reactions.

A similar inhibition protocol was applied to *in situ* experiment and similar result was also observed (Fig. 5(C) and Fig. 5(D)). The obvious decrease of unbinding probability measured in the presence of free GpA molecules demonstrated successful blocking of recognition between PVL on tip and GpA on the cell surface, which provided strong evidence to support the interpretation that a rupture event was coming from breaking of specific interactions between GpA and PVL.

3.4. Force profile analysis for in situ experiment

The internal protein skeletons of erythrocyte govern its distinctive discocyte-echinocyte morphology changes while the transmembrane protein GpA, presenting all of its saccharides to the outside of the cell, can affect the cell shape through direct or indirect association with internal cytoskeletons. AFM was demonstrated to have the capability for distinguishing membrane proteins with/without cytoskeletal associations by analyzing the obtained force curve profile [14]. The force curves called Type I in [14] featured with tether elongation followed by a snap back to the free position of the cantilever were taken to indicate the absence of association with cytoskeletal components, while Type II force curves which showed additional force peaks to Type I curves, were interpreted to indicate the presence of cytoskeletal associations. The *in situ* force curves obtained in our experiment were sorted into 3 groups according to the above definitions: group 1 (Type I), group 2 (similar to Type II), group 3 (not belonging to Types I or II), with the percentage of relative appearance as 67.6%, 24.2% and 9.2%, respectively. The origin of multipeaks in group 2 curves in this work probably involved rupture events of non-specific adhesion of cantilever with sample surfaces in addition to the breakdown of GpA-cytoskeleton interactions. Consequently, our conservative estimate based on the probability of obtaining group 1 curves of GpA free of interaction with cytoskeletal structure was ~70% and result agrees with the reported fact that about 20–30% of GpA are directly or indirectly associated with membrane cytoskeleton [10,30]. The remaining 70–80% were interpreted to be not directly associated with the cytoskeletal structures [31,32].

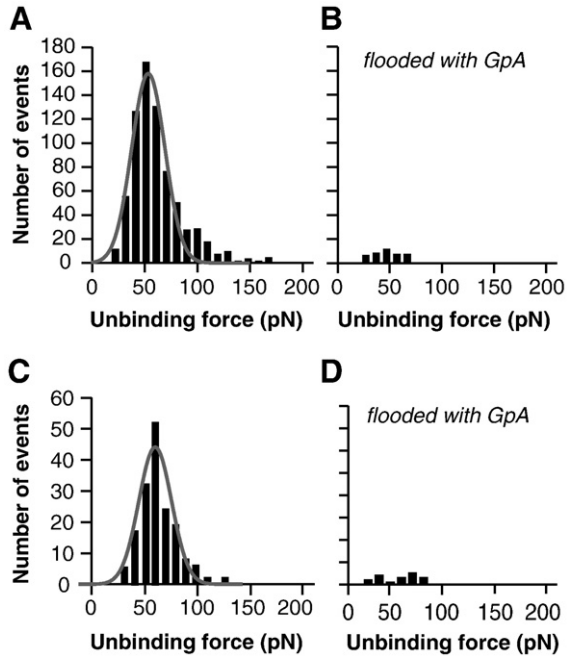

Fig. 5. GpA–PVL binding competitor experiments. (A) Force histogram of GpA–PVL interaction obtained from *in vitro*. (B) As in panel A after tip being blocked with abound free GpA molecules, the unbinding probability was decreased from 46% to 1.22%. (C) Force histogram of GpA–PVL interaction obtained from *in situ*. (D) As in panel C after tip being blocked with abound free GpA molecules, the unbinding probability was decreased from 16.5% to 1.95%.

4. Discussions

We designed the *in vitro* and *in situ* experiments to investigate interactions between GpA and PVL at the single molecular level, and obtained the most probable unbinding force at several loading rates. Based upon the analyzed data we elucidated the dynamic force spectroscopy and energy landscape, and performed force curve profiles analysis.

The multivalency of PVL did not clearly show up in our experiments except that, sometimes, force curves with two or more peaks were observed, which was believed to be due to binding and subsequent unbinding of two or more GpA molecules to PVL modified tip. Whether it was multiple binding to a single lectin molecule or binding to multiple lectin molecules was not confirmed. The *in situ* force curve with a long plateau was considered to be due to the formation of a lipid tether accompanying the pulling process of a transmembrane protein from the membrane [5].

By treating experimental data with Bell-Evans model, we obtained the dynamic force spectroscopy and energy landscape (Fig. 4B). It indicated that the dissociation process of GpA–PVL complex involved overcoming only one energy barrier situated at 0.990 nm from equilibrium. Application of an external force to GpA–PVL complex distorted its energy landscape and lowered the activation barrier [15,33].

Additional experiments were done for both *in vitro* and *in situ* ones to confirm specificity of the binding reaction. GpA–PVL interaction specificity was verified by the unbinding length analysis and inhibition experiment. The unbinding length analysis showed that almost no events were detected beyond an extension of 30 nm (Fig. 2), which was near the longest extreme of PEG linker having an approximate contour length of 32 nm. On the other hand, it indicated that unbinding mainly occurred while PEG linker was not fully stretched. Moreover, inhibition experiments involving binding competitors further demonstrated the specificity of the unbinding reaction we studied. The inhibition was not absolute with limited cases of unbinding events still persisting [22,33–35], for it was mainly coming from a force binding due to the direct contact between tip and sample [27] and it took time for achieving a complete blocking. Reprobing after a relatively longer time greatly decreased the number of persisting events.

The stationary GpA–PVL interaction was studied *in vitro* by BIAcore biosensor and the dissociation constant for GpA–PVL was obtained as 4.3 nM [13], based on which and the value of k_d^0 obtained in this work, the association rate k_a^0 was obtained as 3.3×10^5 mol^{-1} s^{-1}. Comparing with the association rate of 2.0×10^4 mol^{-1} s^{-1} (high-affinity site) or 9.6×10^2 mol^{-1} s^{-1}(low-affinity site) [36] between GpA and wheat germ agglutinin (WGA), which also recognizes the

GlcNAc and Neu5Ac residues in GpA, the association rate between GpA and PVL is at least 16.5-fold larger. This is consistent with the report that GpA reacts with PVL about 50-fold more strongly than WGA [13].

In conclusion, we demonstrated that the interactions between GpA and PVL depended on the loading rate. Force measurement with purified GpA mounted on mica and native GpA on erythrocyte surface fitted well with each other and the most probable force value to break GpA–PVL complex did not depend on molecular environment surrounding GpA *in situ*, indicating that it is possible to analyze GpA-lectin interactions *in vitro* by replacing that *in situ*. Measurement of the interaction between GpA and lectins may help to detect even small changes in the carbohydrate moiety of this glycoprotein [13].

Acknowledgements

We thank Prof. Daocheng Wu for discussions and help. Chao Yan acknowledges the Japan Student Services Organization (JASSO) for financially supporting him through a one-year undergraduate exchange program (Young Scientists Exchange Program 2006–2007) between his home university Xi'an Jiaotong University and host university Tokyo Institute of Technology. This work was supported by a Grant-in-Aid from the Japan Society for the Promotion of Science (JSPS) to RA for Exploratory Research (#19651058) and to AI for Creative Scientific Research (#19GS0418).

References

[1] G.I. Bell, Models for the specific adhesion of cells to cells, Science 200 (1978) 618–627.
[2] L.E. Wybenga, R.F. Epand, S. Nir, J.W. Chu, F.J. Sharom, T.D. Flanagan, R.M. Epand, Glycophorin A is a receptor for Sendai virus, Biochemistry 35 (1996) 9513–9518.
[3] N.H. Tolia, E.J. Enemark, B.K. Sim, L. Joshua-Tor, Structural basis for the EBA-175 erythrocyte invasion pathway of the malaria parasite *Plasmodium falciparum*, Cell 122 (2005) 183–193.
[4] A.L. Cortajarena, F.M. Goni, H. Ostolaza, Glycophorin A is a receptor for *Escherichia coli* alpha-hemolysin in erythrocytes, J. Biol. Chem. 276 (2001) 12513–12519.
[5] H.J. Butt, B. Cappella, M. Kappl, Force measurements with the atomic force microscope: technique, interpretation and applications, Surf. Sci. Rep. 59 (2005) 1–152.
[6] E. Lisowska, Antigenic properties of human glycophorin — an update, Adv. Exp. Med. Biol. 491 (2001) 155–169.
[7] H. Krotkiewski, E. Lisowska, G. Nilsson, G. Gronberg, B. Nilsson, An improved approach to the analysis of the structure of small oligosaccharides of glycoproteins: application to the *O*-linked oligosaccharides from human glycophorin A, Carbohydr. Res. 239 (1993) 35–50.
[8] D.B. Thomas, R.J. Winzler, Structural studies on human erythrocyte glycoproteins, alkali-labile oligosaccharides, J. Biol. Chem. 244 (1969) 5943–5946.
[9] M. Fukuda, M. Lauffenburger, H. Sasaki, M.E. Rogers, A. Dell, Structures of novel sialylated *O*-linked oligosaccharides isolated from human erythrocyte glycophorins, J. Biol. Chem. 262 (1987) 11952–11957.
[10] J.A. Chasis, N. Mohandas, Red blood cell glycophorins, Blood 80 (1992) 1869–1879.
[11] H. Ueda, K. Kojima, T. Saitoh, H. Ogawa, Interaction of a lectin from *Psathyrella velutina* mushroom with *N*-acetylneuraminic acid, FEBS Lett. 448 (1999) 75–80.
[12] H. Ueda, T. Saitoh, K. Kojima, H. Ogawa, Multi-specificity of a *Psathyrella velutina* mushroom lectin: heparin/pectin binding occurs at a site different from the *N*-acetylglucosamine/*N*-acetylneuraminic acid-specific site, J. Biochem. 126 (1999) 530–537.
[13] B. Krotkiewska, M. Pasek, H. Krotkiewski, Interaction of glycophorin A with lectins as measured by surface plasmon resonance, Acta Biochemical Polonica 29 (2002) 481–490.
[14] R. Afrin, A. Ikai, Force profiles of protein pulling with or without cytoskeletal links studied by AFM, Biochem. Biophys. Res. Commun. 348 (2006) 238–244.
[15] E. Evans, K. Ritchie, Dynamic strength of molecular adhesion bonds, Biophys. J. 72 (1997) 1541–1555.
[16] E. Evans, Probing the relation between force-life time and chemistry in single molecular bonds, Annu. Rev. Biophys. Biomol. Struct. 30 (2001) 105–128.
[17] A. Touhami, B. Hoffmann, A. Vasella, F.A. Denis, Y.F. Dufrene, Aggregation of yeast cells: direct measurement of discrete lectin-carbohydrate interactions, Microbiology 149 (2003) 2873–2878.
[18] X. Zhang, D.F. Bogorin, T. Moy, Molecular basis of the dynamic strength of the sialyl Lewis X-selectin interaction, Chemphyschem 5 (2004) 175–182.
[19] E. Thormann, A.C. Simonsen, L.K. Nielsen, O.G. Mouritsen, Ligand-receptor interactions and membrane structure investigated by AFM and time-resolved fluorescence microscopy, J. Mol. Recognit. 20 (2007) 554–560 20.
[20] M. Fukuda, A. Dell, J.E. Oates, M.N. Fukuda, Structure of branched lactosaminoglycan, the carbohydrate moiety of band 3 isolated from adult human erythrocytes, J. Biol. Chem. 259 (1984) 8260–8273.
[21] J.L. Hutter, J. Bechhoefer, Calibration of atomic-force microscope tips, Rev. Sci. Instrum. 64 (1993) 1868–1873.
[22] C. Stroh, H. Wang, R. Bash, B. Ashcroft, J. Nelson, H. Gruber, D. Lohr, S.M. Lindsay, P. Hinterdorfer, Single-molecule recognition imaging microscopy, Proc. Natl. Acad. Sci. U. S. A. 101 (2004) 12503–12507.
[23] C.K. Riener, C.M. Stroh, A. Ebner, C. Klampfl, A.A. Gall, C. Romanin, Y.L. Lyubchenko, P. Hinterdorfer, H.J. Gruber, Simple test system for single molecule recognition force microscopy, Anal. Chim. Acta 479 (2003) 59–75.
[24] S. Kasas, B.M. Riederer, S. Catsicas, B. Cappella, G. Dietler, Fuzzy logic algorithm to extract specific interaction forces from atomic force microscopy data, Rev. Sci. Instrum. 71 (2000) 2082–2086.
[25] C. Ray, J.R. Brown, B.B. Akhremitchev, Correction of systematic errors in single-molecule force spectroscopy with polymeric tethers by atomic force microscopy, J. Phys. Chem. 111 (2007) 1963–1974.
[26] C. Ray, B.B. Akhremitchev, Conformational heterogeneity of surface-grafted amyloidogenic fragments of alpha-synuclein dimers detected by atomic force microscopy, J. Am. Chem. Soc. 127 (2005) 14739–14744.
[27] A. Yersin, T. Osada, A. Ikai, Exploring transferrin-receptor interactions at the single-molecule level, Biophys. J. 94 (2008) 230–240.
[28] H. Ueda, H. Matsumoto, N. Takahashi, H. Ogawa, Psathyrella velutina mushroom lectin exhibits high affinity toward sialoglycoproteins possessing terminal N-acetylneuraminic acid alpha 2,3-linked to penultimate galactose residues of trisialyl N-glycans. Comparison with other sialic acid-specific lectins, J. Biol. Chem. 277 (2007) 24916–24925.
[29] P. Hinterdorfer, W. Baumgartner, H.J. Gruber, K. Schilcher, and H. Schindler. Detection and localization of individual antibody-antigen recognition events by atomic force microscopy, Proc. Natl. Acad. Sci. USA 93 (1996) 3477–3481.
[30] W.C. Hwang, R.E. Waugh, Energy of dissociation of lipid bilayer from the membrane skeleton of red blood cells, Biophys. J. 72 (1997) 2669–2678.
[31] A.R. Anderson, S. Paquette, R. Lovrien, Lectin-erythrocyte interaction with external transmembrane glycophorin saccharides controlling membrane internal cytoskeleta, J. Agric. Food Chem. 50 (2002) 6599–6604.
[32] J.A. Chasis, N. Mohandas, S.B. Shohet, Erythrocyte membrane rigidity induced by glycophorin A-ligand interaction. Evidence for a ligand-induced association between glycophorin A and skeletal proteins, J. Clin. Invest. 75 (1985) 1919–1926.
[33] R. Merkel, P. Nassory, A. Leung, K. Ritchie, E. Evans, Energy landscape of receptor-ligand bonds explored with dynamic fore spectroscopy, Nature 397 (1999) 50–53.
[34] F.W. Bartels, B. Baumgarth, D. Anselmetti, R. Ros, A. Becker, Specific binding of the regulatory protein ExpG to promoter regions of the galactoglucan biosynthesis gene cluster of *Sinorhizobium meliloti* — a combined molecular biology and force spectroscopy investigation, J. Struct. Biol. 143 (2003) 145–152.
[35] R. Ros, F. Schwesinger, D. Anselmetti, M. Kubon, R. Schafer, A. Pluckthun, L. Tiefenauer, Antigen binding forces of individually addressed single-chain Fv antibody molecules, Proc. Natl. Acad. Sci. U. S. A. 95 (1998) 7402–7405.
[36] J.J. Ramsden, C. Schubert Wright, The interaction between wheat germ agglutinin and membrane incorporated glycophorin A. An optical binding study, Glycoconj. J. 12 (1995) 113–121.